Water Science and Engineering, 2010, 3(3): 282-291
doi:10.3882/j.issn.1674-2370.2010.03.004

http://www.waterjournal.cn
e-mail: wse2008@vip.163.com

Geochemical modeling of groundwater in southern plain area of Pengyang County, Ningxia, China

Pei-yue LI*, Hui QIAN, Jian-hua WU, Jia DING

School of Environmental Science and Engineering, Chang'an University, Xi'an 710054, P. R. China

Abstract: The purpose of this paper is to examine the evolution mechanisms of a hydrochemical field and to promote its benefits to the living standards of local people and to the local economy in the southern plain area of Pengyang County, in Ningxia, China. Based on understanding of the hydrogeological conditions in Pengyang County, the chemical evolution characteristics of groundwater in the plain area were analyzed. PHREEQC geochemical modeling software was used to perform hydrochemical modeling of water-rock interaction and to quantitatively analyze the evolution processes and the formation mechanisms of the local groundwater. Geochemical modeling was performed for two groundwater paths. The results showed that, along path 1, Na^+ adsorption played the leading role in the precipitation process and its amount was the largest, up to 6.08 mmol/L; cation exchange was significant along path 1, while along simulated path 2, albite accounted for the largest amount of dissolution, reaching 9.06 mmol/L, and the cation exchange was not significant. According to the modeling results, along the groundwater flow path, calcite and dolomite showed oversaturated status with a precipitation trend, while the fluorite and gypsum throughout the simulated path were not saturated and showed a dissolution trend. The total dissolved solids (TDS) increased and water quality worsened along the flow path. The dissolution reactions of albite, CO_2, and halite, the exchange adsorption reaction of Na^+, and the precipitation of sodium montmorillonite and calcite were the primary hydrogeochemical reactions, resulting in changes of hydrochemical ingredients.

Key words: *hydrogeochemistry; water-rock reaction; groundwater modeling; Pengyang County*

1 Introduction

In typical arid and semiarid areas, groundwater is the major source of water for most uses (Al-Shaibani 2008). The chemistry of groundwater is an essential parameter for assessing the environmental characteristics of an area (Park et al. 2005; Gallardo and Tase 2007). The main factors affecting water quality changes are lithofacies geographical conditions, groundwater recharge and runoff conditions, and the degree of openness of groundwater systems (Xu et al. 2009). Hydrogeochemistry has been one of the hot research topics in recent years. Geochemical modeling, mostly known as inverse modeling, which is a useful tool for studying

This work was supported by the National Natural Science Foundation of China (Grant No. 40772160), the Research on Drinking Water Environment and Endemic in Villages and Small Towns in New Socialist Countryside Project (Grant No. 010) supported by the Ningxia Land and Resources Department, and the Program of Introducing Talents of Discipline to Universities (111 Project) (Grant No. B08039).
*Corresponding author (e-mail: *lipy2@163.com*)
Received Mar. 1, 2010; accepted Jun. 16, 2010

hydrochemical evolution, is commonly used to reconstruct geochemical evolution of groundwater from one point in an aquifer to another point located in the inverse direction along the groundwater flow path (Sharif et al. 2008; Wang et al. 2010). Geochemical modeling has been used by many scholars and researchers around the world in various fields. Abu-Jaber and Ismail (2003) used the geochemical mass-balance technique to quantify the contribution of different sources, geochemical processes, and rock types to the final water composition, applying the NETPATH software package in the northern Jordan Valley. Lecomte et al. (2005) simulated the weathering reactions in the Los Reartes River Basin by means of PHREEQC inverse modeling and examined the factors controlling montane weathering. Bertolo et al. (2006) investigated the hydrochemistry of a thick unsaturated zone in a tropical region in Urânia, São Paulo State, in Brazil. In their study, they determined geochemical processes in the unsaturated zone and explained the factors affecting shallow groundwater chemistry. Martens et al. (2010) simulated extraction tests on cement-waste samples with a thermodynamic equilibrium model using a consistent database. They modeled subsequent diffusion tests by means of a three-dimensional diffusive transport model combined with the geochemical model derived from the extraction tests.

In Pengyang County, endemic fluorosis disease has been seriously endangering the health of local residents. The availability and quality of groundwater resources in the area have been closely related to the local economic development and people's living standards, therefore, it is necessary to carry out hydrochemical field research. In this study, the authors applied hydrogeochemical theory to groundwater hydrochemical field research with water quality analysis data to explain the formation conditions of the modern hydrochemical field, to explore the formation and migration patterns of groundwater in the plain area, and to provide a basis for the establishment of a groundwater system model of the plain area. In addition, underground water-rock interaction studies have theoretical and practical significance for identifying characteristics of groundwater enrichment and groundwater recharge, runoff, and discharge conditions, as well as for evaluating the long-term potential for the development of regional groundwater resources, and for promoting social and economic development and ecological environmental protection and governance in the region (Xu et al. 2009).

2 General conditions of study area

Pengyang County is situated in southern Ningxia Hui Autonomous Region, east of the Liupan Mountains, between longitude 106°32'E and 106°58'E, and latitude 35°4l'N and 36°17'N. The area is 62 km long from north to south, and 58 km wide from east to west, and covers 3241.1 km^2. The southern plain area is home to most local people and situated in the southern Ruhe River and Honghe River Valley regions, which were formed by river alluvium. The study area is shown in Fig. 1.

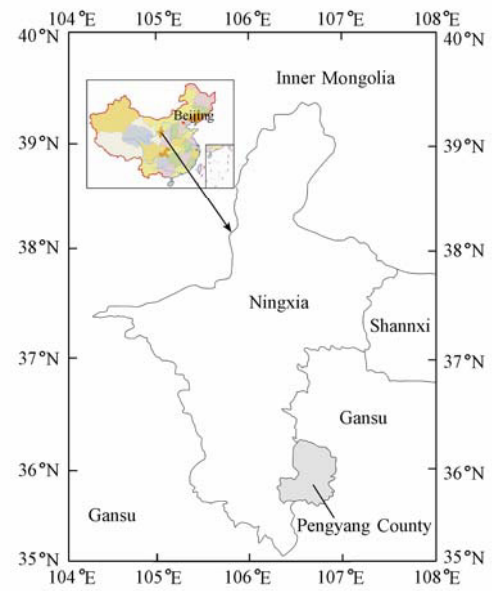

Fig.1 Location of study area

The aquifers here contain a large amount of groundwater, which constitutes the main water source in the area. Landscape types in the region are dominated by medium and low mountains, loess hills, and river valley terraces. Multi-year mean rainfall is about 500 mm in the area. Annual precipitation is mainly concentrated in July, August, and September, and the total precipitation of those three months accounts for nearly 60% of the total precipitation over the whole year. Groundwater pH values vary between 7.85 and 8.36, and are hence a bit alkaline. The exposed rock strata are mainly Cretaceous sandstone, Tertiary sandstone, muddy siltstone, and Quaternary alluvial and proluvial deposits. Rock minerals usually include feldspar, quartz, calcite, dolomite, gypsum, fluorspar, and sodium montmorillonite (Qian et al. 2009). The major rivers, the Ruhe River and Honghe River, lie in the south of the county. The alluvial plains are formed by the rivers, and the lithology of the Quaternary alluvial layer shows a dual structure: the upper part is sticky sand and the lower part is sand and gravel with greater thickness, containing more groundwater. The major cation in the groundwater is Na^+, followed by Mg^{2+} and Ca^{2+}; major anions are HCO_3^- and SO_4^{2-}, followed by Cl^-. Hydrochemical types are mostly the $HCO_3 \cdot SO_4$-Na·Mg·Ca type and the $HCO_3 \cdot SO_4$-Na·Mg type. The water is of a comparatively fine quality and is fit for drinking. The Quaternary sand and gravel aquifer is the main water-bearing formation for the water supply in the area and is also the layer of interest in this study. The major source of groundwater recharge in the area is precipitation. After recharge, groundwater runs from both sides of the river to the river valley in a horizontal direction, and along the river valley from upstream to downstream in a vertical direction. Discharge to the river and artificial exploitation are the main discharge modes.

3 Materials and theoretical basis

3.1 Materials

Representative water samples were collected from 33 shallow monitoring wells (depths were usually 10-20 m) in August 2007. Sampling locations are shown in Fig. 2. Samples were collected in pre-cleaned plastic polyethylene bottles for physicochemical analysis. Prior to sampling, all the sampling containers were washed and rinsed thoroughly with the groundwater to be taken for analysis. Each of the groundwater samples was analyzed for 26 parameters, including carbonate, bicarbonate, chloride, sulphate, phosphate, calcium, magnesium, sodium,

kalium, pH, chemical oxygen demand (COD), total dissolved solids (TDS), total hardness (TH), nitrate, ammonia nitrogen, fluoride, total iron (Tfe), total alkalinity, total acidity, chroma, arsenic, iodine, aluminum, nitrite, metasillicio acid, and free carbon dioxide, by the laboratory of the Ningxia Geological and Environmental Monitoring Station. During sample collection, handling, and preservation, standard procedures recommended by the Chinese Ministry of Water Resources were followed to ensure data quality and consistency.

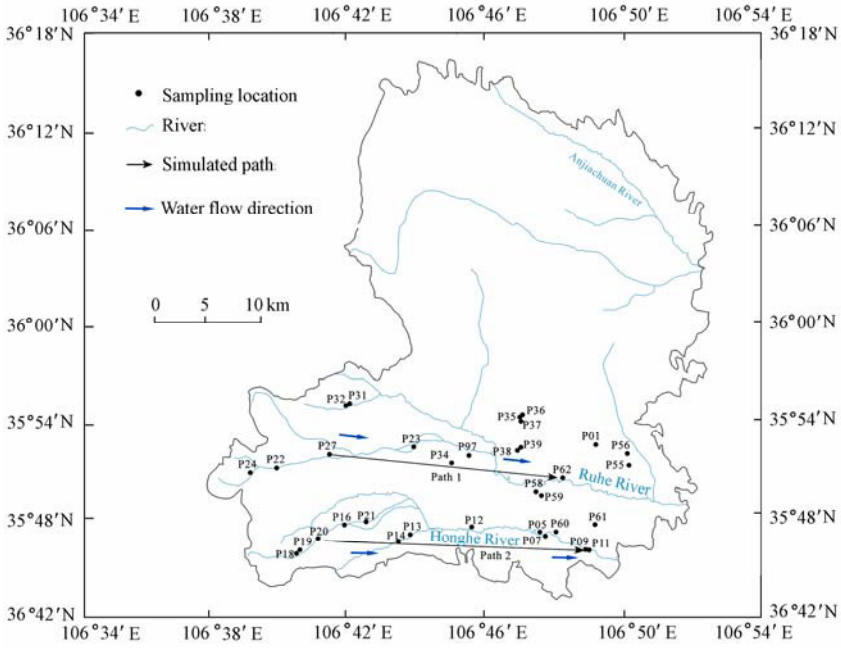

Fig. 2 Sampling locations in study area

3.2 Saturation index

The saturation index (S_I) is a widely used indicator in hydrogeochemical study. It describes the saturation status of minerals in the groundwater. When $S_I = 0$, the minerals in the aqueous solution are in equilibrium status; when $S_I < 0$, the minerals in the aqueous solution have not reached saturation, and bear on a dissolution trend; when $S_I > 0$, a supersaturated status of minerals in the aqueous solution is indicated and mineral deposition will occur (Qian and Ma 2005; Luo et al. 2008). The saturation index (S_I) is defined as

$$S_I = \lg \frac{I_{AP}}{K} \tag{1}$$

where I_{AP} is the relevant ion activity product in a mineral dissolution reaction, which can be obtained by multiplying the ion activity coefficient γ_i and composition concentration m_i; and K is the equilibrium constant of mineral dissolution at a certain temperature.

3.3 Mass balance simulation

Mass balance simulation, which determines the amount of dissolved or deposited

minerals and gases at two points along the groundwater flow line, is mainly used to study chemical reactions taking place along the groundwater flow line and to analyze groundwater hydrochemical composition changes according to the chemical reactions in groundwater, solids, and gases (Qian and Ma 2005). The key concepts and terminology used in constructing net geochemical mass-balance reactions are constraints, phases, and models (Abu-Jaber and Ismail 2003). The mass balance simulation method has been described as follows:

Two samples collected from two different points along the groundwater flow path are determined; the water quality at the upstream point is considered the initial water quality, and the water quality at the downstream point the end water quality. Then, the principle of geochemical mass-balance reactions can be described as follows: the sum of the initial aqueous components and reactants equals to the sum of the end aqueous components and resultants.

Under general circumstances, mass balance simulations are carried out against the elements. If n elements in the aqueous solution are considered, the amount of dissolution or deposition of n minerals can be determined by the mass balance simulation:

$$\sum_{j=1}^{n} a_{ij} x_j = b_i \tag{2}$$

where a_{ij} is the stoichiometric number of the ith element in relation to the jth mineral, a dimensionless value equal to the molar number of ith element generated by the complete dissolution of 1 mol of jth mineral; x_j is the molar number that the jth mineral precipitates or dissolves (positive for dissolution, and negative for precipitation); and b_i is the increment of the ith element in the end water quality.

Note that the possible mineral phase identified in the reactions is a set of ambiguous phases; it refers to the selected chemical elements according to the reactants and the resultant in a given hydrogeological system (Xu et al. 2009).

4 Simulated paths and possible mineral phases

Hydrogeochemical modeling requires that water sampling points be in the same water flow path (Luo et al. 2008). Therefore, two simulated paths from west to east were determined according to the groundwater flow. Path 1 was from point P27 to point P62; P27 was located in the upper reaches of the Ruhe River Plain, and P62 was located at the downstream site. Path 2 was from point P20 to point P11; P20 was located in the upper reaches of the Honghe River plain, and P11 was located in the downstream section. The two paths are shown in Fig. 2.

The main criteria for the selection of the possible mineral phase are measurement and analysis of aquifer minerals, groundwater chemical composition, and conditions of groundwater occurrence (Gao 2005; Luo et al. 2008). The main chemical elements contained in the selected possible mineral phase should be in accordance with the compositions detected in the groundwater (Gao 2005). According to water quality analysis results, the major cation in the studied groundwater is Na^+, followed by Ca^{2+} and Mg^{2+}. HCO_3^- and SO_4^{2-} are the major anions, followed by Cl^-. Based on the water quality analysis results, halite, sodium

montmorillonite, calcite, dolomite, and gypsum should be the main mineral constituents of aquifers. In order to study the role of fluorine in geochemistry, fluorite was considered a possible mineral phase. In addition, because the water samples were all taken from an unconfined aquifer, CO_2 was included in the possible mineral phase.

The role of cation exchange in the groundwater is of great significance in the evolution of hydrochemical composition. Whether the ion-exchange reaction occurs or not can be determined by the trend of the milligram equivalent concentration ratio of Ca^{2+} to Na^+ ($N(Ca^{2+})/N(Na^+)$) from the initial water sample to the end water sample. If $N(Ca^{2+})/N(Na^+)$ decreases, Ca^{2+} in the water may be undergoing exchange with Na^+ in the clay. If $N(Ca^{2+})/N(Na^+)$ increases, there may be exchange between Na^+ in the water and Ca^{2+} in the clay (Sun et al. 2007; Luo et al. 2008). From the $N(Ca^{2+})/N(Na^+)$ variation diagrams (Fig. 3) we can see that $N(Ca^{2+})/N(Na^+)$ shows an upward trend along path 1, but a downward trend along path 2. Therefore, the process of cation exchange may occur during groundwater flow along both path 1 and path 2.

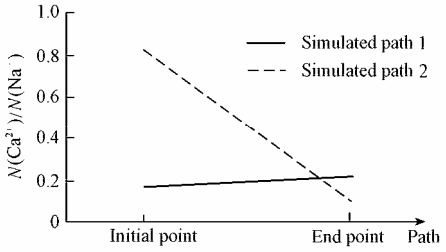

Fig. 3 $N(Ca^{2+})/N(Na^+)$ variations in simulated paths

In summary, the possible mineral phase in the study area was determined to include gypsum, sodium montmorillonite, fluorite, calcite, halite, dolomite, CO_2, albite, and K-feldspar, as well as cation exchange. Table 1 shows the specific reaction equations.

Table 1 Equations of mineral (gas) dissolution

Mineral	Equation of mineral (gas) dissolution
Gypsum	$CaSO_4{\cdot}2H_2O = Ca^{2+} + SO_4^{2-} + 2H_2O$
Sodium montmorillonite	$3Na_{0.33}Al_{2.33}Si_{3.67}O_{10}(OH)_2 + 30H_2O + 6OH^- = Na^+ + 7Al(OH)_4^- + 11H_4SiO_4$
Fluorite	$CaF_2 = Ca^{2+} + 2F^-$
Calcite	$CaCO_3 = Ca^{2+} + CO_3^{2-}$
Halite	$NaCl = Na^+ + Cl^-$
Dolomite	$CaMg(CO_3)_2 = Ca^{2+} + Mg^{2+} + 2CO_3^{2-}$
CO_2	$CO_2 + H_2O = H_2CO_3$
Albite	$NaAlSi_3O_8 + 8H_2O = Na^+ + Al(OH)_4^- + 3H_4SiO_4$
K-feldspar	$KAlSi_3O_8 + 8H_2O = K^+ + Al(OH)_4^- + 3H_4SiO_4$
Cation exchange	$2NaX + Ca^{2+} \leftrightarrow 2Na^+ + CaX_2$

5 Results and discussion

5.1 Calculation of saturation index

For the minerals (gases), the saturation index method was used to analyze the dissolution or precipitation trend. For the reactive minerals, including sodium montmorillonite, halite,

sodium feldspar, and K-feldspar, because of the great solubility and low concentrations in groundwater, these minerals were unsaturated with dissolved trends. To study the dissolution or precipitation trends of gypsum, fluorite, calcite, and dolomite, saturation indexes were calculated according to the results of chemical analysis which listed in Table 2. The results of the saturation index are listed in Table 3.

Table2 Water quality analysis results along simulated paths

No.	Mass concentration (mg/L)											pH
	Na^+	K^+	Mg^{2+}	Ca^{2+}	Cl^-	SO_4^{2-}	HCO_3^-	F^-	CO_2	H_2SiO_3	TDS	
P27	171.50	2.10	80.72	50.86	62.14	320.37	489.14	2.00	6.49	12.80	947.96	8.09
P62	212.00	4.00	52.23	78.24	186.41	353.31	301.01	0.70	6.78	17.70	1 057.81	8.03
P20	44.00	1.50	30.86	62.59	20.71	89.96	329.09	0.12	6.49	14.40	427.07	8.09
P11	272.00	4.00	54.60	46.94	124.27	359.80	514.22	1.40	4.45	14.60	1 133.32	8.02

Table 3 Saturation index along simulated paths

Mineral	Saturation index			
	Simulated path 1		Simulated path 2	
	P27	P62	P20	P11
Calcite	0.808	0.721	0.808	0.717
Fluorite	–0.270	–1.000	–2.522	–0.625
Dolomite	2.137	1.586	1.621	1.820
Gypsum	–1.171	–0.948	–1.496	–1.169

From Table 3 we can see that the minerals along simulated path 1 had the same precipitation or dissolution trend as those along simulated path 2. Calcite and dolomite along the simulated paths showed supersaturated status with a precipitation trend, while the fluorite and gypsum throughout the simulation were unsaturated with a dissolution trend. According to water quality analysis results, on simulated path 1, the TDS of water samples at the initial point was 947.96 mg/L, and it increased to 1 057.81 mg/L at the end point of the water sample. The hydrochemical type varied from the HCO_3·SO_4-Na·Mg type to the SO_4·Cl·HCO_3-Na type, which shows that from west to east, and from upstream to downstream, corrosion effects are significant and water quality gradually deteriorates. Along simulated path 2, the TDS varied from 427.07 mg/L at the initial point to 1 133.32 mg/L at the end point, and the hydrochemical type was the HCO_3·SO_4-Ca·Mg·Na type at the initial point and changed to the HCO_3·SO_4-Na·Mg type at the end point, which also indicates that dissolution effects along simulated path 2 are strong and water quality gradually deteriorates.

5.2 Mass balance simulation

PHREEQC (Parkhurst and Appelo 1999), a hydrogeochemical modeling software, was applied to the possible mineral phase in the mass balance simulation to calculate the amount of various minerals dissolved or precipitated in the simulated paths, and the calculation results

are shown in Table 4.

Table 4 Calculation results of amount of minerals dissolved or precipitated

Path	Amount of minerals dissolved or precipitated (mmol/L)										
	Gypsum	Sodium montmorillonite	Fluorite	Calcite	Halite	Dolomite	CO_2	Albite	K-feldspar	NaX	CaX_2
Path 1	0.34	–4.89	–0.07	–1.44	3.50	–1.19	0.73	5.95	0.05	–6.08	3.04
Path 2	2.81	–7.45	0.07	–4.06	2.92	0.99	5.12	9.06	0.06	0.40	–0.20

Note: positive for dissolution, negative for precipitation.

From the mass balance simulation results we can see that dissolution of albite, halite, gypsum, K-feldspar, and CO_2 took place along simulated path 1. At the same time, cation exchange between Na^+ and Ca^{2+} occurred. During this process, Na^+ from the halite and albite dissolved into the water then underwent exchange with Ca^{2+} absorbed on the rock surface. Ca^{2+} from the rock surface dissolved into the water, and Na^+ was adsorbed into the rock surface. Na^+ adsorption reaction played the leading role in the precipitation process and its precipitation amount was the largest, up to 6.08 mmol/L, followed by sodium montmorillonite, calcite, and dolomite, with amounts of 4.89 mmol/L, 1.44 mmol/L, and 1.19 mmol/L, respectively. Along the flow path line, the concentrations of Na^+, Cl^-, K^+, and SO_4^{2-} gradually increased because of the increasing dissolution effects of halite, albite, K-feldspar, and gypsum, respectively, while the reduction of Mg^{2+} and F^- could respectively be attributed to the precipitation of dolomite and fluorite. The increase in the concentrations of Na^+, Cl^-, and SO_4^{2-}, as well as the reduction in the concentrations of Mg^{2+} and HCO_3^-, caused the groundwater hydrochemical type to change from the $HCO_3 \cdot SO_4$-Na·Mg type to the $SO_4 \cdot Cl \cdot HCO_3$-Na type. Generally speaking, albite dissolution should have left a large amount of $Al(OH)_4^-$ and SiO_2 in the groundwater, but the water quality analysis results showed that the content of Si did not increase significantly and the element content of Al was nearly zero. Taking into account a large amount of precipitations of sodium montmorillonite, we have sufficient reason to believe that $Al(OH)_4^-$ and SiO_2, along with the relevant ions in the aqueous solution, formed the sodium montmorillonite; that is to say, the dissolution of albite led to the precipitation of sodium montmorillonite, which is a common albite weathering result in nature. The dissolved CO_2 caused the water pH value to decrease, promoting the dissolution of gypsum. Cation exchange and the dissolution of gypsum caused the increase of Ca^{2+} in the water body, which then caused calcite, dolomite, and fluorite precipitation. From the calculation results we can see that on simulated path 1 the cation exchange reaction was relatively strong, but the concentration variations of Ca^{2+} and Na^+ were not large, and the $N(Ca^{2+})/N(Na^+)$ trend was not significant. This indicates that the dissolution effects of albite and halite were roughly equal to the precipitation effects of sodium montmorillonite and ion exchange, and the precipitation of calcite and dolomite was roughly equal to the effects of ion exchange reactions.

On simulated path 2, albite accounted for the largest amount of dissolution, reaching 9.06 mmol/L, followed by the dissolution of CO_2, which was 5.12 mmol/L. At the same time,

halite, gypsum, dolomite, fluorite, and K-feldspar also dissolved on different levels, and the cation exchange reactions between Na^+ and Ca^{2+} also occurred along simulated path 2. Sodium montmorillonite accounted for the largest amount of precipitation, 7.45 mmol/L, followed by calcite, with 4.06 mmol/L. Along the water flow path, CO_2 dissolved in large volume, coupled with the dissolution of dolomite, which together made the concentration of HCO_3^- increase, caused the reduction of the pH, and in turn promoted the dissolution of gypsum. Similar to the case of simulated path 1, large amounts of albite dissolved, which theoretically should have left a large amount of $Al(OH)_4^-$ and SiO_2 in the groundwater. However, for the same reasons as with path 1, they were quickly converted into sodium montmorillonite, which meant that albite dissolution led to the precipitation of sodium montmorillonite. Gypsum and dolomite dissolution in the aqueous solution should have caused a noticeable increase in Ca^{2+}, whereas in fact the content of Ca^{2+} decreased. After analysis we found that, in addition to cation exchange, a large amount of calcite precipitation occurred. Thus, we came to the assumption that Ca^{2+} and CO_3^{2-} together formed calcite; that is to say, gypsum and dolomite caused calcite precipitation, and large amounts of Mg^{2+} and SO_4^{2-} were left in the water. Increase in the concentration of Na^+ and Mg^{2+}, together with the reduction of Ca^{2+}, caused the groundwater hydrochemical types to change from the HCO_3·SO_4-Ca·Mg·Na type to the HCO_3·SO_4-Na·Mg type. Fluorite dissolution caused the F^- content to increase in the water, which was consistent with the results of water quality analysis. According to the water quality analysis results and simulation results, we determined that the cation exchange had no significant effects along path 2. The concentration of Na^+ increased, Ca^{2+} did not significantly decrease in volume, and $N(Ca^{2+})/N(Na^+)$ showed a clear downward trend, which helped us draw the conclusions that the dissolution effects of halite and albite were far greater than the precipitation effects of sodium montmorillonite, and the calcite precipitation effects were slightly more significant than the dissolution of gypsum and dolomite.

6 Conclusions

Through hydrogeochemical modeling theory and methods, water-rock interactions in the southern plain of Pengyang County were simulated and examined, and the following conclusions were drawn:

(1) Minerals examined in the paper along simulated path 1 showed the same dissolution or deposition trend as those along simulated path 2. Throughout the simulation, calcite and dolomite showed oversaturated status with a precipitation trend, while the fluorite and gypsum throughout the simulated path were not saturated and showed a dissolution trend.

(2) The TDS gradually increases from upstream to downstream in the plain area, and the water quality gradually deteriorates. Along simulated path 1, the dissolution of albite and halite, the absorption of Na^+, and the precipitation of sodium montmorillonite are the major phenomena, and cation exchange is significant on path 1. On simulated path 2, the dissolution of albite, CO_2, and halite, and the precipitation of calcite and sodium montmorillonite are the

main phenomena, and the dissolution of albite and halite is much more significant than the precipitation of sodium montmorillonite. The precipitation of calcite is slightly more significant than the dissolution of gypsum and dolomite, while the cation exchange is not significant along path 2. The changes in groundwater chemical composition result from the combined actions of aforementioned dissolutions and precipitations, as well as cation exchange reactions.

References

Abu-Jaber, N., and Ismail, M. 2003. Hydrogeochemical modeling of the shallow groundwater in the northern Jordan Valley. *Environmental Geology*, 44(4), 391-399. [doi:10.1007/s00254-003-0770-9]

Al-Shaibani, A. M. 2008. Hydrogeology and hydrochemistry of a shallow alluvial aquifer, Western Saudi Arabia. *Hydrogeology Journal*, 16(1), 155-165. [doi:10.1007/s10040-007-0220-y]

Bertolo, R., Hirata, R., and Sracek, O. 2006. Geochemistry and geochemical modeling of unsaturated zone in a tropical region in Urânia, São Paulo state, Brazil. *Journal of Hydrology*, 329(1-2), 49-62. [doi:10.1016/j.jhydrol.2006.02.001]

Gallardo, A. H., and Tase, N. 2007. Hydrogeology and geochemical characterization of groundwater in a typical small-scale agricultural area of Japan. *Journal of Asian Earth Sciences*, 29(1), 18-28. [doi:10.1016/j.jseaes.2005.12.005]

Gao, W. B. 2005. *Application of Inverse Simulation Method in Groundwater Evolution of Huanhe Group in the Ordos Basin*. Ph. D. Dissertation. Xi'an: Chang'an University. (in Chinese)

Lecomte, K. L., Pasquini, A. I., and Depetris, P. J. 2005. Mineral weathering in a semiarid mountain river: Its assessment through PHREEQC inverse modeling. *Aquatic Geochemistry*, 11(2), 173-194. [doi: 10.1007/s10498-004-3523-9]

Luo, Q. B., Kang, W. D., Xie, Y. L., and Zhao, B. F. 2008. Groundwater hydrogeochemistry simulation in the Jingbian area of the Luohe of Cretaceous. *Ground Water*, 30(6), 22-24. (in Chinese)

Martens, E., Jacques, D., Van Gerven, T., Wang, L., and Mallants, D. 2010. Geochemical modeling of leaching of Ca, Mg, Al, and Pb from cementitious waste forms. *Cement and Concrete Research*, 40(8), 1298-1305. [doi:10.1016/j.cemconres.2010.01.007]

Park, S. C., Yun, S. T., Chae, G. T., Yoo, I. S., Shin, K. S., Heo, C. H., and Lee, S. K. 2005. Regional hydrochemical study on salinization of coastal aquifers, western coastal area of South Korea. *Journal of Hydrology*, 313(3-4), 182-194. [doi:10.1016/j.jhydrol.2005.03.001]

Parkhurst, D. L., and Appelo, C. A. J. 1999. *User's Guide to PHREEQC (Version 2)-A Computer Program for Speciation, Batch-Reaction, One-Dimensional Transport, and Inverse Geochemical Calculations*. Denver: U. S. Geological Survey Earth Science Information Center.

Qian, H., and Ma, Z. Y. 2005. *Hydrogeochemistry*. Beijing: Geological Publishing House. (in Chinese)

Qian, H., Zhang, Q., Zhu, L. S., Li, P. Y., Song, B. D., Wei, Y. N., and Chen, J. 2009. *Report on Drinking Water Environment and Endemic Investigation in New Socialist Countryside of Pengyang*. Yinchuan: Ningxia Geological and Environmental Monitoring Station. (in Chinese)

Sharif, M. U., Davis, R. K., Steele, K. F., Kim, B., Kresse, T. M., and Fazio, J. A. 2008. Inverse geochemical modeling of groundwater evolution with emphasis on arsenic in the Mississippi River Valley alluvial aquifer, Arkansas (USA). *Journal of Hydrology*, 350(1-2), 41-55. [doi:10.1016/j.jhydrol.2007.11.027]

Sun, Y. Q., Qian, H., and Wu, X. H. 2007. Hydrogeochemical characteristics of groundwater depression cones in Yinchuan City, Northwest China. *Chinese Journal of Geochemistry*, 26(4), 350-355. [doi:10.1007/s11631-007-0350-x]

Wang, P. M., Anderko, A., Springer, R. D., Kosinski, J. J., and Lencka, M. M. 2010. Modeling chemical and phase equilibria in geochemical systems using a speciation-based model. *Journal of Geochemical Exploration*, 106(1-3), 219-225. [doi:10.1016/j.gexplo.2009.09.003]

Xu, Z. H., Li, Y. F., Jiang, L., Hou, G. C., and Hu, A. Y. 2009. Geochemical modeling of Huanhe water-bearing layers in South Ordos Basin. *Journal of Arid Land Resources and Environment*, 23(9), 160-168. (in Chinese)